









Pushing the boundaries
of chemistry?
It takes
#HumanChemistry

Make your curiosity and talent as a chemist matter to the world with a specialty chemicals leader. Together, we combine cutting-edge science with engineering expertise to create solutions that answer real-world problems. Find out how our approach to technology creates more opportunities for growth, and see what chemistry can do for you at:

evonik.com/career



The in-vitro biocompatibility of ureido-pyrimidinone compounds and polymer degradation products

Paul J. Besseling¹  | Tristan Mes² | Anton W. Bosman² | Joris W. Peeters³ |
Henk M. Janssen^{3,4} | Maarten H. Bakker⁵ | Joost O. Fledderus¹  |
Martin Teraa¹  | Marianne C. Verhaar¹  | Hendrik Gremmels¹  |
Patricia Y. W. Dankers^{4,5} 

¹Department of Nephrology and Hypertension, University Medical Center Utrecht, Utrecht, The Netherlands

²SupraPolix BV, Eindhoven, The Netherlands

³SyMO-Chem BV, Den Dolech 2, Eindhoven, The Netherlands

⁴Department of Biomedical Engineering, Laboratory of Chemical Biology, Eindhoven University of Technology, Eindhoven, The Netherlands

⁵Institute for Complex Molecular Systems, Eindhoven University of Technology, Eindhoven, The Netherlands

Correspondence

Prof. Patricia Y.W. Dankers, Institute for Complex Molecular Systems, Eindhoven University of Technology, Postbus 513, 5600 MB Eindhoven, The Netherlands.
Email: p.y.w.dankers@tue.nl

Funding information

Ministerie van Onderwijs, Cultuur en Wetenschap, Grant/Award Number: 024.001.035; ZonMw, Grant/Award Number: 436001003

Abstract

Supramolecular biomaterials based on ureido-pyrimidinone (UPy) moieties are versatile polymer materials as their function can be tailored to the application. These UPy-materials can be designed into polymer coatings, self-healing polymers, hydrogels and elastomers. The biocompatibility of UPy-based materials and their degradation products is a long-term success requirement for many regenerative medicine and biomedical applications. Earlier research has shown that UPy-based materials and polymers display no immediate toxic effects, but in-depth in-vitro studies on potential UPy-polymer degradation products have not been executed. Owing to their resemblance to naturally occurring purines and pyrimidines, UPy-compounds and their degradation products could potentially initiate an immune response or be mutagenic. Accordingly, 11 selected UPy-compounds were synthesized, and their effect on cell viability, wound healing, and their immunogenicity and potential mutagenic potential, were studied. We showed that low molecular weight degradation products of UPy-based biomaterials do not affect cell viability, nor do these interfere with several aspects of endothelial function including proliferation, angiogenic sprouting and cellular migration even in levels exceeding plausibly attainable concentrations. Furthermore, the compounds are neither immunogenic nor mutagenic, showing that UPy-biomaterials exhibit good biocompatibility in vitro, and could in principle be used in humans.

KEYWORDS

in-vitro biocompatibility, polymer degradation products, supramolecular biomaterials, ureido-pyrimidinone (UPy)

1 | INTRODUCTION

Supramolecular materials are composed of small molecules, oligomers or macromolecules that are held together via directed non-covalent interactions such as hydrogen bonds, metal–ligand coordination or charge–charge interactions.¹ The supramolecular interactions between the (macro)molecules in large part determine the properties of the materials. Owing to the presence of these directed non-covalent interactions supramolecular materials can be easily tuned with respect to their specific properties (e.g., biodegradability, [non]-cell adhesion, or mechanical properties). One of the most promising classes of supramolecular polymer materials is based on quadruple hydrogen bonding ureido-pyrimidinone (UPy) moieties, which are particularly suitable for producing bioactive materials due to their formation of dynamic bio-active bioresorbable elastomeric materials.² As the intended application of these materials is to form degradable scaffolds and hydrogels in in-situ tissue engineering applications, requirements for biocompatibility are greater than for conventional materials.

This can be done by mixing-in (bio)molecules of choice, provided these (bio)molecules are also decorated with the particular non-covalently interacting sub-unit.^{3–6} Their wide-ranging modular capacity in addition to their biodegradability provides potential in a broad range of applications, for example as scaffolds in the field of tissue engineering, that is, vascular grafts,⁷ heart valves,⁸ renal membranes,⁹ prolapse meshes,¹⁰ and as drug delivery vehicles in vivo.^{11,12}

Previously, no acute cytotoxic effects of UPy-based polymer materials have been reported^{2,13} However, the employed assays are not suitable to detect subtle interferences of the material with cellular function. Furthermore, engrafting cells *in vivo* are not only exposed to intact UPy-based polymer materials, but also to their soluble degradation products. UPy-based materials have been successfully used in in-vivo studies, predominantly focusing on material properties^{2,3,11} and have been investigated for the foreign body reaction or specific cell infiltration/adhesion properties.^{4,10}

Here, we investigated the potential effects of possible UPy-degradation products of UPy-polymers (Figure 1) on various aspects of cellular functioning using in-vitro assays. The enzymatic degradation pathways for UPy-polycaprolactone scaffolds have been shown to be predominantly oxidative and to a much lesser effect hydrolytic.¹⁴ To test the biocompatibility, we have investigated several aspects of the multifactorial process of tissue engineering and wound repair. Our primary focus was on the effects of UPy-degradation products on endothelial colony forming cells (ECFC) cells and leukocytes, as these

two cell classes would form the interface between an implanted construct and the recipient organism. We simulated various steps of endothelial progenitor cell engraftment in an engineered construct, including acute toxicity, proliferation, migration and angiogenesis. In addition, we examined activation and reactive oxygen species production by leukocytes in response to soluble UPy-degradation products and possible mutagenic effects.

2 | EXPERIMENTAL SECTION

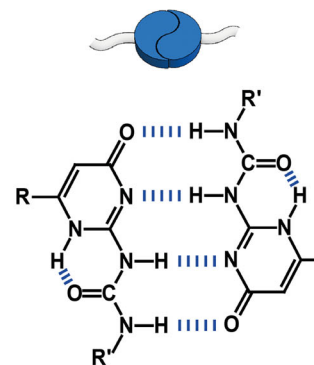
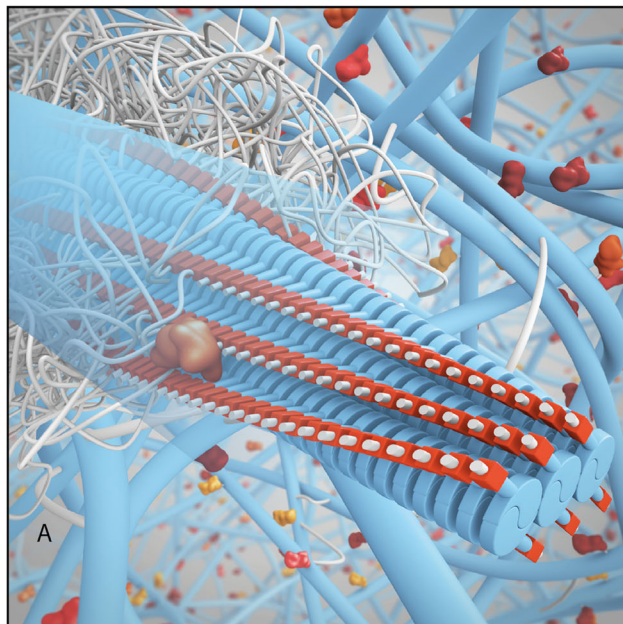
2.1 | Synthesis

UPy-amine **1** was obtained by acid hydrolysis of its 6-isocyanato precursor, whereas UPy diamine **2** was obtained after reaction of a carbonyldiimidazole activated hydroxyethyl-functional isocytosine with an excess 1,6-hexanediamine. Dicarboxylate UPy **3** was obtained from the functionalization of UPy **2** with carbonyldiimidazole activated 6-hydroxyhexanoic ester followed by deprotection. Isocytosine **4** was obtained by coupling mono-Boc-protected 1,6-hexanediamine with a carbonyldiimidazole activated hydroxyethyl-functional isocytosine derivative followed by acid hydrolysis of the Boc-group. UPy-derivative **5** resulted from the reaction of carbonyldiimidazole activated t-butyl ester functional isocytosine **6** with mono-Boc-protected 1,6-hexanediamine, followed by acid hydrolysis of the Boc-groups. Whereas, carboxylic acid functional isocytosine **6** was obtained from the condensation of guanidine carbonate with a t-butyl ester functional β -keto-ester followed by acid hydrolysis. UPy diol **7** was obtained from the coupling of UPy **2** with carbonyldiimidazole activated mono-tetrahydropyranyl(THP) protected hexanediol followed by acid hydrolysis. Elaborate synthesis procedures and analyses for compounds **1–7** are given in the Supplementary Information. Compounds **8**, **9**, **10**¹⁵ and **11**,¹⁶ have been synthesized according to literature procedures. All compounds were dissolved in DMSO (Sigma Aldrich) and stored at -20°C before the different biocompatibility tests.

2.2 | Cell isolation and culture

Human umbilical cord blood was collected from full term pregnancies, using a protocol approved by the local ethics committee (METC, University Medical Center Utrecht [UCMU]; protocol number 01/230 K).¹⁷ Mononuclear cells (MNCs) were isolated by density gradient centrifugation using Ficoll-paque (GE Healthcare, density

(A)



(B)

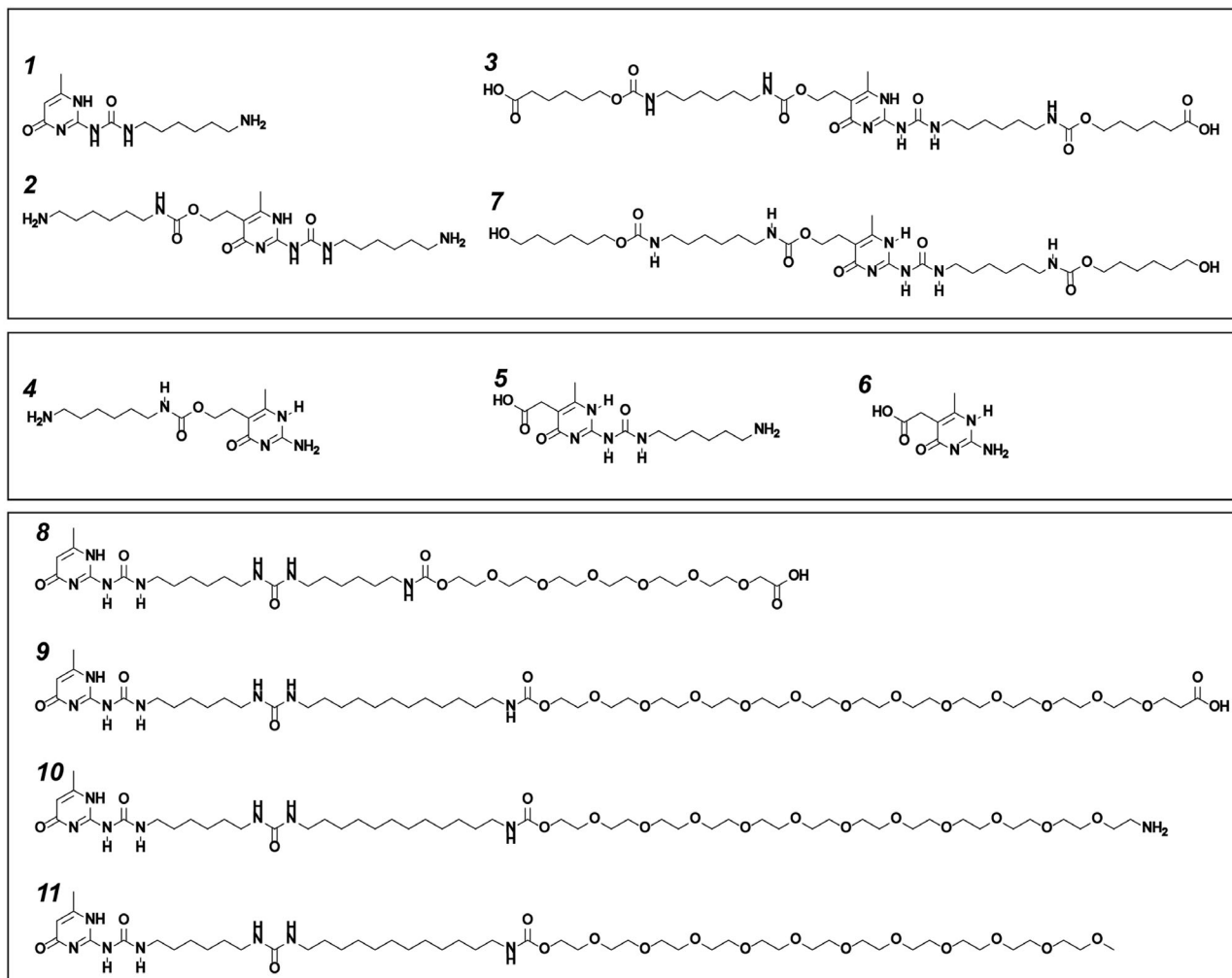


FIGURE 1 Schematic representation and chemical structures of ureido-pyrimidinone (UPy) biomaterials. (A) Supramolecular UPy-biomaterials can be formed by mixing supramolecular polymers with (bio)active additives. The UPy-units dimerize via quadruple hydrogen bonding. (B) UPy-derivatives (1, 2, 3, 5, 7) and isocytosine derivatives (4 and 6) which can be formed upon hydrolytic or oxidative degradation of polycaprolactone- or polycarbonate-based UPy-scaffolds, and UPy-oligo(ethylene glycol) derivatives (8, 9, 10, 11), which may form upon degradation of peptide bioactives or supramolecular hydrogelators as prepared from UPy-building blocks [Color figure can be viewed at wileyonlinelibrary.com]

1.077 g/ml). MNCs were subsequently resuspended in Endothelial Growth Medium-2 (EGM-2) containing SingleQuots (Lonza, Walkersville, MD, USA), 10% fetal calf serum (FCS), and 100 units/100 µg penicillin/streptomycin per ml and seeded on Collagen I (BD Biosciences, Heidelberg, Germany) coated wells at a density of $2 \cdot 10^6$ cells per cm^2 and cultured at 37 °C, 5% CO_2 in a humidified incubator. After 24 h, non-adherent cells were aspirated and complete EGM-2 medium was added to each well. Medium was changed three times per week thereafter. Cells were harvested when colonies appeared and expanded for further use. All experiments were conducted with cell passages 3–5, and multiple donor isolates were used for each experiment as indicated in the Figure legends.

2.3 | Flow cytometric characterization of ECFCs

Cells were harvested by trypsinization and labeled with the following antibodies: anti-hVEGFR2-PE (R&D Systems FAB357P), anti-hCD34-FITC (BD pharmingen 555,821), anti-CD31-PE (BD pharmingen 555,446), anti-CD90-PE (R&D Systems FAB2067P), anti-CD105-PE (Biolegend 135,506) anti-CD45-PE (BD pharmingen 557,748), and anti-CD14-PE (DAKO R0864), anti-CD146-A647 (Biolegend 361,013) or anti-CD133-PE (Miltenyi Biotec 130–080-801). The following isotype controls (BioLegend) were used: PE-conjugated Rat IgG2ak (RTK2758), FITC-conjugated Rat IgG2bk (RTK4530), A647-conjugated (400130) and PE-Cy7. Antibody labeling was performed for 30 min at 4 °C in the presence of FcR-Blocking reagent (Miltenyi Biotec 130–059-901). Subsequently the cells were washed twice using PBS. Sytox® Blue (Life Technologies, Bleiswijk, The Netherlands) was added directly before each measurement in order to assess viability. Flow-cytometric analysis ($\geq 10^4$ events acquired) was performed using a Becton Dickinson FACSCanto II. (Figure S1).

2.4 | Mutagenicity

For measuring possible mutagenic properties, we conducted an AMES fluctuation test as described by Sui et al.¹⁸ Tester strains (*S. typhimurium*) TA98 (hisD3052/rfa/DuvrB/pKM101) and TA100 (hisG46/rfa/DuvrB/pKM101) in STDiscs™ were acquired from Moltox® and grown in Oxoid™ Nutrient Broth No. 2 containing ampicillin. Overnight cultures of TA98 and TA100 strains were cultured until $\text{OD}_{600} = 1$. Strains were exposed for 90 min to compounds in a 24-well plate and

where incubated at 37 °C in a shaking incubator (200 RPM). After exposure, 2.5 ml of indicator medium was added to each well of the 24-well plate containing the reaction mixture. Using 8-channel micropipette 50 µl of the reaction mixture in one well of the 24-well plate was transferred into 48 wells of a 384-well plate. The 384-well plates were sealed in Ziplock™ plastic bags to prevent evaporation and incubated for 72 h at 37 °C in a shaking incubator (200 RPM). Positive wells in which the color changed from purple to yellow were counted manually. Positive wells turn yellow due to the fermentation of glucose to an acid product, while the negative wells remain purple. The percent of positive wells for each dose and the positive control was calculated. Positive controls for TA98 and TA100 were respectively 2-Nitrofluorene (2NF, 2 µg/ml) and 4-Nitroquinoline 1-oxide (4NQO, 0.5 µg/ml). Solvent control contained 1:100 DMSO.

2.5 | Cell viability

Analysis of cell proliferation and cytotoxicity was done by AlamarBlue® assay. ECFCs were seeded into 96-well plates at a density of 10^4 /well. After 24 h growth, 50 µl EGM-2 with a concentration range of compounds was added to the wells in quadruple and incubated for 2 h in a humidified incubator at 37 °C, 5% CO_2 . AlamarBlue® was added and after 30 min baseline measurements were established. After further 24 h incubation fluorescence at 570 nm (Ex: 530 nm) was measured. A known cytostatic drug (Doxorubicin) was used as a positive control.

2.6 | Cell proliferation

The xCELLigence® RTCA DP device (ACEA Bioscience, Inc., San Diego, USA) uses noninvasive electrical impedance monitoring to quantify cell proliferation in a real-time manner. Measurements were carried out according to manufacturer's instructions. The dimensionless parameter termed Cell index (CI) displays the relative change in the measured electrical impedance. The CI reflects restrictions in ionic movement and conductance between electrodes by cellular plasma membranes and is directly proportional to the cell count and cell adhesion. A serial dilution of the compounds was added to the in 16-well-E-plates (ACEA Biosciences, Inc) in a total volume of 100 µl per well, with an added solvent control of 1:50 DMSO. After a 30 min calibration at RM temp and sequentially blanking of the machine; 2500 ECFCs were seeded in a volume of 100 µl. The E-plates were placed in

a RTCA DP analyzer and incubated at 37 °C, 5% CO₂ in a humidified incubator and monitored for up to 96 h. Proliferation rate was calculated as a rolling slope as shown in.¹⁹

2.7 | Wound healing

To assess the horizontal ECFC migration and response to damage signals, a scratch-wound assay was performed as in.²⁰ ECFCs were grown until confluence in a 24-well plate. A scratch in the monolayer was made using a 20 to 200 µl pipette tip, detached cells were washed off, and a concentration range of compounds was added to the wells in quadruple. As a negative control bare EBM-2 (no growth factors or serum) was added to the wells. Photographs were made on demarcated reference points at baseline and $t = 6$ h. The average scratch width per high-powered field was calculated by dividing the area of the scratch by the length of the scratch, and migration was subsequently calculated by subtracting the width at baseline by the width at $t = 6$ h and normalized for full medium control.

2.8 | Sprouting assay

Angiogenic sprouting was determined by seeding ECFCs on matrigel in a well of an IBIDI µ-slide angiogenesis (IBIDI, Martinsried, Germany). Wells were filled with 10 µl growth factor-reduced Matrigel (BD), 40 µl EGM-2 containing a concentration range of compound was dispensed on top of the solidified Matrigel. The 3000–5000 cells suspended in 10 µl EGM-2 were added. As a negative control bare EBM-2 was used instead of EGM-2. Cells were allowed to form tubular networks for 6 h, after which photographs were taken. Each sample was photographed and automated (Photoshop script) chosen fields (1300 by 1300 px) were analyzed with the Angiogenesis Analyzer for ImageJ.²¹

2.9 | Phagocyte activation

Phagocyte activation was measured with a PHAGOBURST™ kit (BD),²² which is a quantitative determination of leukocyte oxidative burst in whole blood (WB). EDTA WB was obtained from the Mini Donor Service (MDD) at the UMCU, The Netherlands (METC UMCU; protocol number 07-125/C). For clearer separation of the monocyte population, cells were labeled with anti-CD14-PE (DAKO R0864). Unlabeled

opsonized bacteria (*E. coli*), phorbol 12-myristate 13-acetate (PMA) and the chemotactic peptide N-formyl-Met-Leu-Phe (fMLP) were used as stimulants and dihydrorhodamine (DHR) 123 as a fluorogenic substrate. The evaluation of oxidative burst activity was performed by flow cytometry with the use of a FACSCANTO II (BD) and analyzed by Flowjo®.

2.10 | Statistical analysis

Data is reported as the mean \pm SEM ($n \geq 3$). Statistical analysis was performed using GraphPad Prism version 7.00 for Windows. Means of experimental data were compared by One-way ANOVA followed by Dunnett's multiple comparisons test and differences were considered statistically significant for $p < 0.05$.

3 | RESULTS AND DISCUSSION

3.1 | UPy-compound design

Nine different UPy-derivatives and two isocytosine-based metabolites were synthesized (Figure 1). We propose that these compounds are present in the degradation products of UPy-elastomer polymers based on polycaprolactone or poly(hexylcarbonate) (Compounds 1–7) or part of the UPy-poly(ethylene glycol) hydrogel form we often used (compounds 8–11). Compounds 1, 2, 3, and 6 could originate from enzymatic hydrolysis by cholesterol esterases or lipases in line with previous findings on hydrolysis of ester, urethane, and carbonate bonds in polyurethanes.²³ Oxidative degradation pathways could lead to compounds 1–7, due to abstraction by oxygen radicals of β -methylene protons at the ester, carbonate, urethane or urea, which after chain scission will ultimately lead to the formation of alcohol groups (from carbonate), carboxylate groups (from carbonate, ester, urethane), or amine groups (from urethane, urea).²⁴ The relationships between these degradation compounds, their parent UPy-polymers, and degradation pathways are given in Table 1.

TABLE 1 Possible origins of degradation products

UPy-polymer	Degradation pathway	
	Hydrolysis	Oxidative
Polycaprolactone based	1, 2, 3, 4	1, 2, 3, 4, 5, 6
Polycarbonate based	1, 2, 4, 7	1, 2, 3, 4, 5, 6, 7
Poly(ethylene glycol) based	1, 8, 9, 10	1, 8, 9, 10

3.2 | Endothelial Colony forming cells characterization

By making use of ECFCs, primary endothelial progenitor cells with de novo vessel-forming capacity, our model resembles the in-vivo situation with a cell source that will be exposed to a high level of scaffold breakdown products in circulation. Cultured ECFCs organized into their characteristic colonies with rounded cell morphology and exhibited a cobblestone morphology when passaging. The cultured ECFCs were immunophenotyped using flow cytometry (Figure S1). Characteristic for the endothelial profile of ECFCs; cells were found positive for the endothelial markers CD31, CD146 and VEGFR2, progenitor marker CD105, variable expression of CD34 and negative for the myeloid markers CD14, CD45 and CD133.

3.3 | Mutagenicity

One of the primary conditions for using materials in vivo is that these are not mutagenic. To test for potential mutagenicity of our compounds, we performed an Ames

fluctuation test with two histidine dependent strains TA98 and TA100. Known mutagens (2-Nitrofluorene and 4-Nitroquinoline-N-oxide respectively) specific for these strains were used as positive controls which showed an average of 99% and 50% positive wells. Indicating a clear mutagenic potential when compared to the solvent controls ($p < 0.0001$). Samples from the UPy-compounds with concentrations as high as 100 μ M showed no significant difference compared to solvent control in both strains, indicating no mutagenic potential of these compounds or their degradation products (Table S1).

3.4 | Cell viability

The UPy-backbone shows structural similarities to purine and pyrimidine nucleobases. We hypothesized that they might behave similarly to known cytostatic drugs such as 5-Fluorouracil²⁵ and thiopurines,²⁶ which are known to act as a pseudosubstrate and can be mistaken for a nucleotide during DNA repair or replication, leading to misincorporation and possible cytotoxicity. To test for this possible cytotoxicity, an AlamarBlue® assay was performed. Doxorubicin, a known cytostatic drug, was used

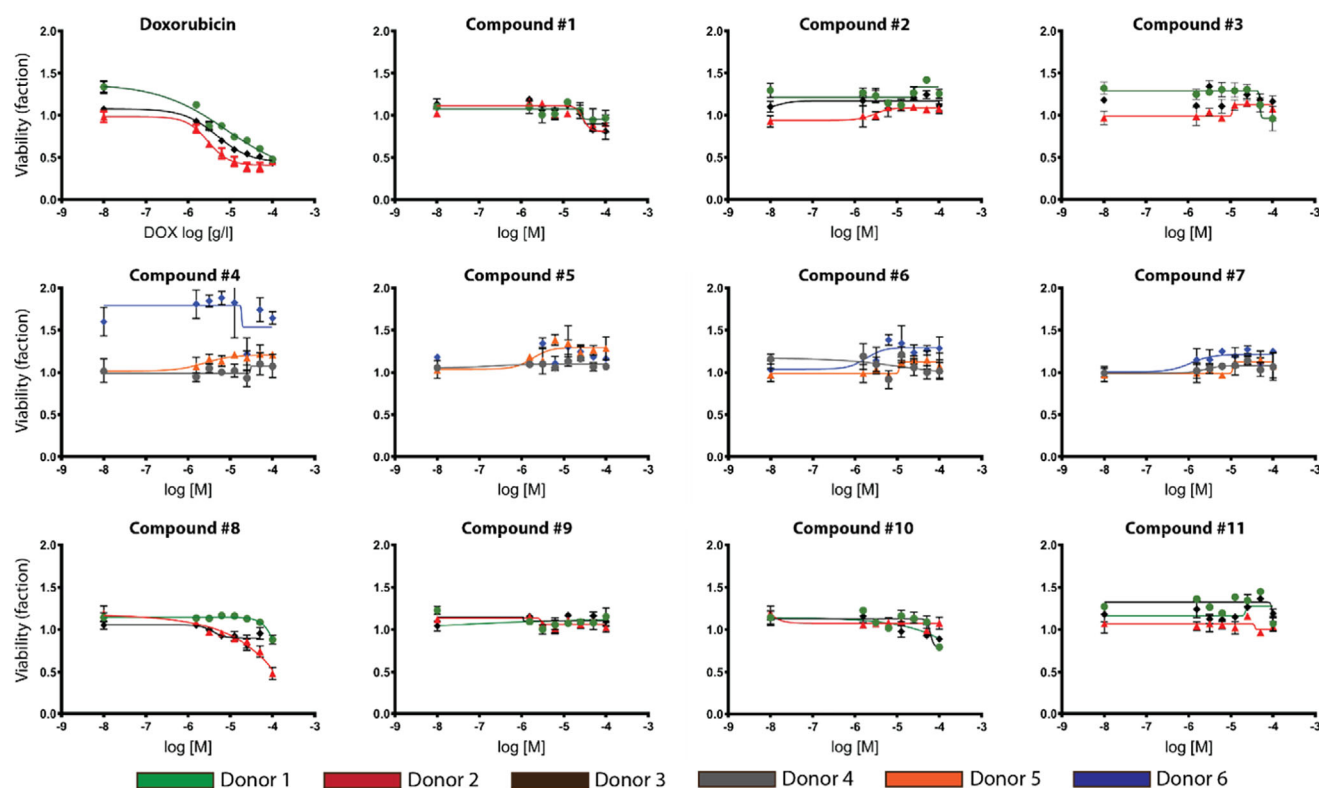


FIGURE 2 ECFC viability using AlamarBlue assay on samples with a 2 h exposure to UPy-compounds, all tested samples normalized to full medium control (set to 1). Doxorubicin (DOX) was used a positive control to simulate dose dependent decrease in cell viability. Experiment was done independently and with at least three donors. The data was quantified as the mean \pm SEM with (where possible) a non-linear four parameter dose response curve fit [Color figure can be viewed at wileyonlinelibrary.com]

as a positive control and showed a dose dependent decrease in ECFC viability compared to untreated cells with an IC_{50} of $5.4 \pm 1.6 \mu\text{M}$. All UPy compound-treated conditions showed no dose-dependent inhibition up to a concentration of $100 \mu\text{M}$ (Figure 2). In order to obtain these high concentrations of all compounds, we were limited by the hydrophobic properties of the UPy-compounds, which required the need for organic solvents, such as DMSO, which is toxic to cells. This is illustrated by the non-dose response effect seen in the viability studies with compounds **8** and **10** (which reached up to 1:20 and 1:50 DMSO levels, respectively). Overall, we can conclude, in spite of their resemblance to purine and pyrimidine nucleobases, that there is no negative influence of our compounds on ECFC viability.

3.5 | Cell proliferation

Another possible effect of misincorporation is a disrupted cell proliferation, which is tightly linked to DNA replication. To investigate this, we assessed real-time proliferation of ECFCs exposed to compound sample dilutions

(ranging from 1.56 to $100 \mu\text{M}$) over 72 h using the cellular impedance based xCELLigence® system (Figure 3). Proliferation rates were calculated as the maximum slope (Figure S3) and normalized to the solvent control. Although no overall adverse effects and no related cell death were observed, a rapid decrease in measured impedance to below zero with $100 \mu\text{M}$ of compound **10** was found, which could point at a significant decrease in proliferation rate. However, we propose this is due to interference with the electric impedance measurements at these high concentrations, possibly linked to the low solubility of the compound (similar levels of organic solvent were used with compound **8**). No significant decrease in proliferation was found in the dilutions up to $50 \mu\text{M}$ of compound **10** and all the other compounds up to $100 \mu\text{M}$. Considering the hydrophobic nature of the UPy moiety, it must be noted that the compound is not soluble in aqueous solutions at this concentration without the presence of a solvent, making it unlikely that cells will be exposed to such high concentrations (μM levels) *in vivo*. Indicating that there is no significant influence of our compounds on the proliferation rate of ECFCs.

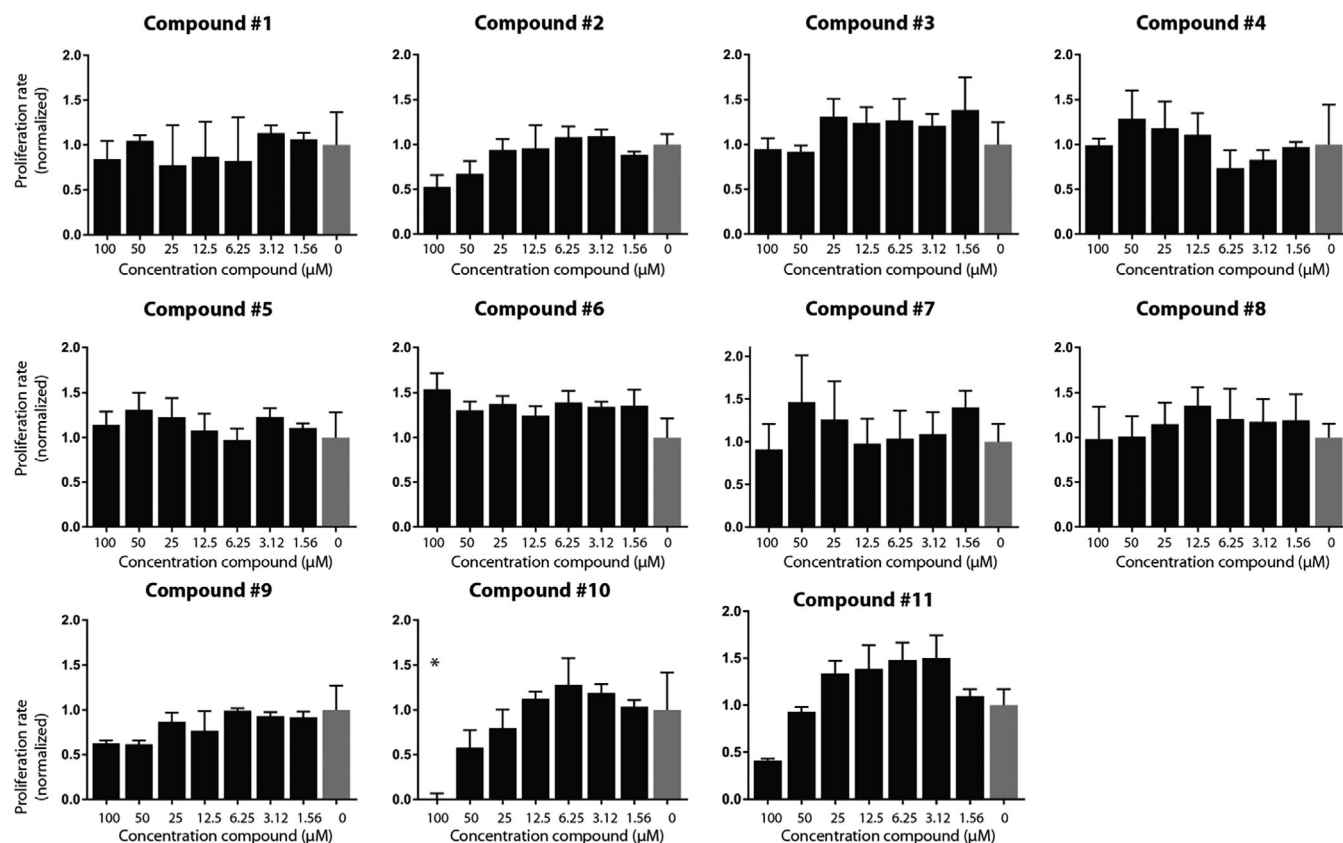


FIGURE 3 ECFC proliferation rate measured with xCELLigence. Proliferation rate consists of the maximum slope and normalized to the vehicle control (1:100 DMSO). Experiment was done independently and with at least three donors. The data was quantified as the mean \pm SEM. * $p < 0.05$

3.6 | Cell migration

Cell migration is an essential process in wound healing and/or de novo tissue formation.²⁷ A scratch assay with ECFCs was performed to assess the influence of UPy-compounds on endothelial cell migration (Figure 4). Sample dilutions up to 25 μ M were used and wound closure after 6 h was normalized to the full medium control with 1:100 DMSO. The negative control of bare medium (no FCS and growth factors) showed a significant difference in fractional closure ($p < 0.05$). In comparison, no significant difference in wound closure was observed of our compound dilutions compared to full medium ($p \geq 0.91$), indicating no inhibitory effect on endothelial cell migration.

3.7 | Angiogenesis

Additionally, angiogenesis is also an essential component of tissue repair or tissue formation.²⁸ Analogs of the purines adenine²⁹ and guanine³⁰ have been shown to

stimulate or inhibit angiogenesis through activation or inhibition of the adenosine A1 receptor. To test the effect on angiogenic capacity of ECFC, we performed a sprouting assay on matrigel and measured the branching interval of the formed sprouts (Figure 5). We found a significant ($p < 0.01$) difference in branch interval between the full medium positive control (148.8 ± 17.6 px) and the no-growth-factor negative control (54.6 ± 9.4 px), but in UPy-compound treated conditions we observed formation of typical endothelial tubules and no significant difference compared to the positive control with a branch interval ranging from 88.68 ± 9.5 px to 178 ± 45.93 px ($p \geq 0.87$). These results indicate that there is no inhibitory effect on the angiogenic capacity of our endothelial cells caused by our UPy compounds.

3.8 | Immune cell activation

Activation of phagocytic cells is important in tissue remodeling, but can also cause collateral damage of host

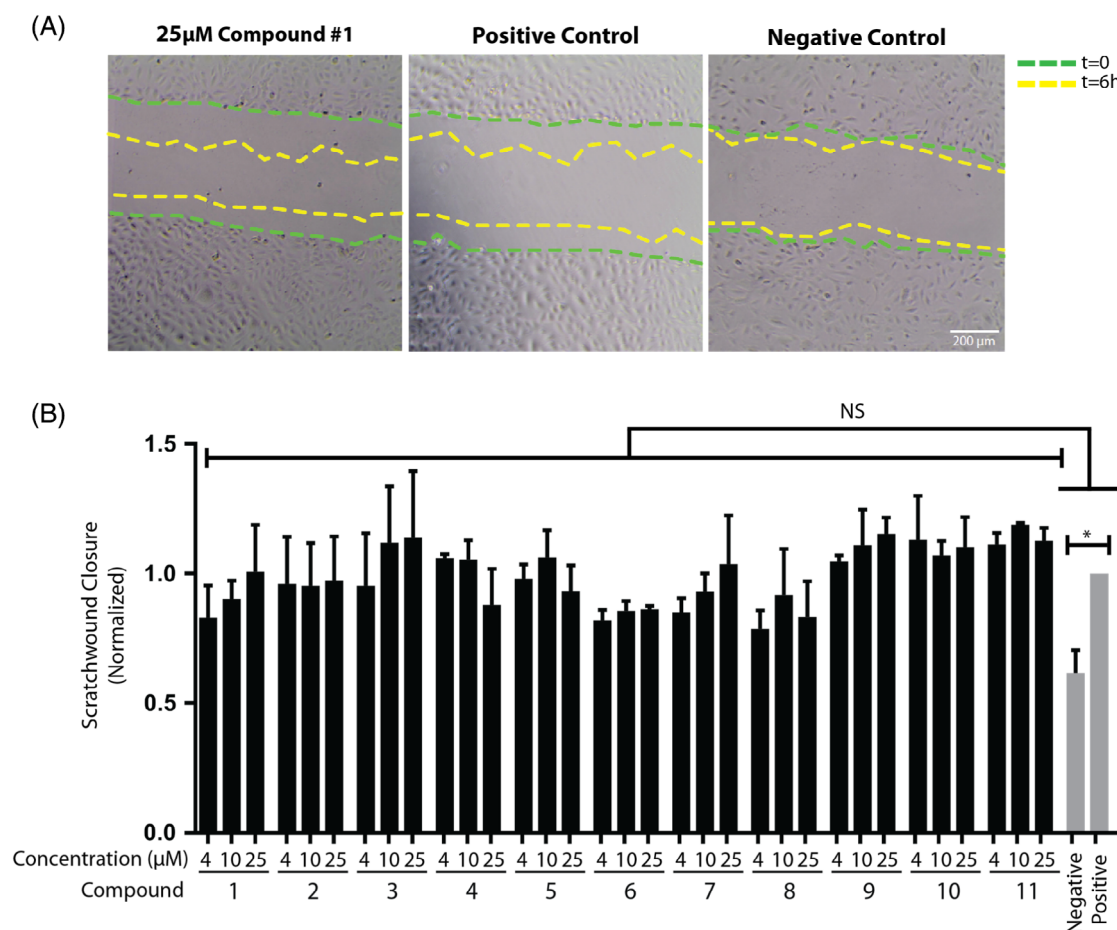


FIGURE 4 Wound healing scratch assay. (A). Representative photographs 6 h after scratch wounding of a confluent ECFCs layer, treated with a UPy-compound, full medium and bare medium-controls. (B). Each sample was photographed and closure fraction was quantified compared to the positive control. Each experiment was done independently and with at least three donors. The data was quantified as the mean \pm SEM with a one-way ANOVA and Dunnett's multiple comparison tests. * p value < 0.05 negative control: EBM-2, without growth factors and FCS. Positive control: Full medium +10% FCS [Color figure can be viewed at wileyonlinelibrary.com]

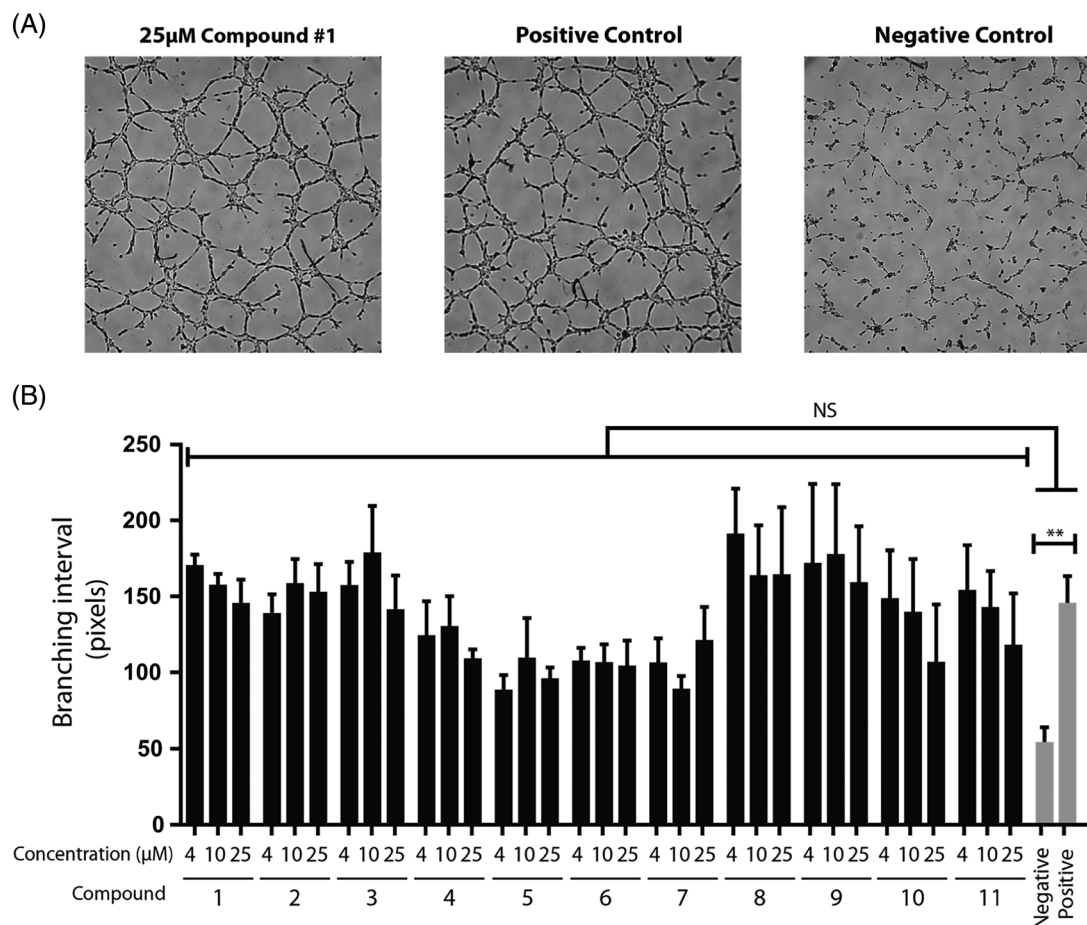


FIGURE 5 Matrigel sprouting assay. (A) Representative photographs of sprouting endothelial colony forming cells (ECFCs) when treated, untreated and bare medium-controls. Each sample was photographed and the branching interval was quantified in automated chosen fields and (B) normalized to the positive control. The data was quantified as the mean \pm SEM with a one-way ANOVA and Dunnett's multiple comparison tests, $n = 3$ donors. ** p value < 0.01 compared with the positive control group. Negative control: EBM-2, without growth factors and serum. Positive control: Full medium +10% FCS

tissues and over activation may results in fibrous encapsulation, linking it to poor biocompatibility and biofouling.³¹ To test the possible capacity of UPy-compounds to activate an oxidative burst in phagocytes cells and thereby induce an immune response we conducted a Phagoburst™ assay. Granulocyte and monocyte populations from whole blood were sorted as shown in Figure S3. Activation of these populations were assessed by measuring the oxidation of dihydrorhodamine 123 by flow cytometry as shown in Figure 6(A). PMA and *E. coli* positive controls both caused a significant ($p < 0.0001$) oxidative burst, showing an average of 97% and 85% oxidative burst in granulocytes and 45% and 36% oxidative burst in monocytes respectively. Non-significant activation was observed compared to the wash control, when we subjugated the whole blood samples to UPy-compounds (up to 25 μ M) or the low activator fMLP (Figure 6(A)-(C)). No significant activation of

oxidative burst in phagocytic cells in reaction to our UPy-compounds was observed. However, due to the essential character of the immune system in tissue formation and remodeling, the long-term effects on the immune system should be closely monitored in further in vivo studies.

4 | CONCLUSION

The in-vitro results support the biocompatibility of UPy-materials in a diversity of processes involved in the systemic reaction to implanted UPy-polymer biomaterials. This renders UPy-materials promising candidates for future applications in in-situ bioengineered scaffolds or in controlled (drug) delivery models. Importantly, future (long-term) in-vivo studies should further support the biocompatibility results of the current study.

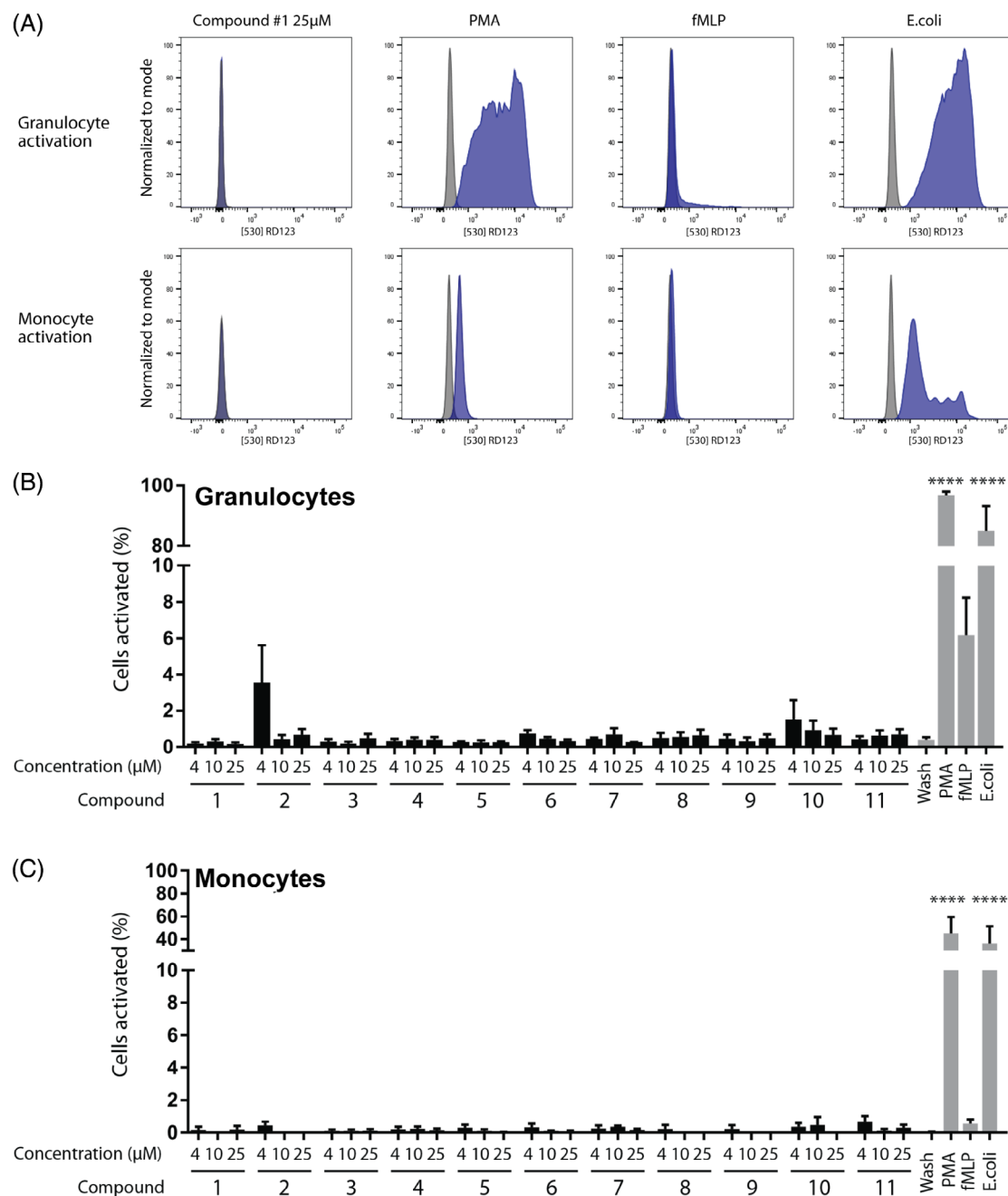


FIGURE 6 Oxidative burst assay (A) Histograms of RD123 intensity under different conditions compared to wash. Phagocytosis and oxidative burst of (B) granulocytes and (C) monocytes was measured by flow cytometry after ex-vivo exposure of whole blood with 4 μ M, 10 μ M or 25 μ M of UPy-compounds in addition to the controls consisting of wash buffer, phorbol 12-myristate 13-acetate (PMA) and the chemotactic peptide N-formyl-met-Leu-Phe(fMLP) and *E. coli*. Each experiment was done independently and with at least three donors. The data is shown as the mean \pm SEM and compared to wash control **** $p < 0.0001$ [Color figure can be viewed at wileyonlinelibrary.com]

ACKNOWLEDGMENTS

This work was financially supported by the European Research Council (FP7/2007-2013) ERC Grant Agreement 308045, and the Ministry of Education, Culture and Science (Gravity program 024.001.035). Also, the InSiTeVx project is acknowledged (project number 436001003), that is financially supported by ZonMw within the LSH 2Treat program and the Nierstichting.

CONFLICT OF INTEREST


No conflicts of interest reported.

DATA AVAILABILITY STATEMENT

The datasets generated during and/or analysed during the current study are available from the corresponding author on reasonable request.


ORCID

Paul J. Besseling  <https://orcid.org/0000-0002-5636-6277>

Joost O. Fledderus  <https://orcid.org/0000-0002-7353-2572>

Martin Teraa  <https://orcid.org/0000-0002-6751-6752>

Marianne C. Verhaar  <https://orcid.org/0000-0002-3276-6428>

Hendrik Gremmels  <https://orcid.org/0000-0002-7818-620X>

Patricia Y. W. Dankers  <https://orcid.org/0000-0002-8997-181X>

REFERENCES

- [1] T. Aida, E. W. Meijer, S. I. Stupp, *Science* **2012**, 335, 813.
- [2] P. Y. W. Dankers, M. C. Harmsen, L. A. Brouwer, M. J. A. van Luyn, E. W. Meijer, *Nat. Mater.* **2005**, 4, 568.
- [3] D. E. P. Muylaert, G. C. van Almen, H. Talacua, J. O. Fledderus, J. Kluin, S. I. S. Hendrikse, J. L. J. van Dongen, E. Sijbesma, A. W. Bosman, T. Mes, S. H. Thakkar, A. I. P. M. Smits, C. V. C. Bouten, P. Y. W. Dankers, M. C. Verhaar, *Biomaterials* **2016**, 76, 187.
- [4] G. C. Van Almen, H. Talacua, B. D. Ippel, B. B. Mollet, M. Ramaekers, M. Simonet, A. I. P. M. Smits, C. V. C. Bouten, J. Kluin, P. Y. W. Dankers, *Macromol. Biosci.* **2016**, 16, 350.
- [5] O. J. G. M. Goor, H. M. Keizer, A. L. Bruinen, M. G. J. Schmitz, R. M. Versteegen, H. M. Janssen, R. M. A. Heeren, P. Y. W. Dankers, *Adv. Mater.* **2017**, 29, 1.
- [6] B. D. Ippel, B. D. Ippel, M. I. Komil, M. I. Komil, P. A. A. Bartels, P. A. A. Bartels, S. H. M. Söntjens, R. J. E. A. Boonen, R. J. E. A. Boonen, M. M. J. Smulders, P. Y. W. Dankers, P. Y. W. Dankers, P. Y. W. Dankers, *Macromolecules* **2020**, 53, 4454.
- [7] H. Talacua, A. I. P. Smits, D. E. P. Muylaert, J. W. van Rijswijk, A. Vink, M. C. Verhaar, A. Driessen-Mol, L. a. van Herwerden, C. V. C. Bouten, J. Kluin, F. P. T. Baaijens, *Tissue Eng. Part A* **2015**, 21, 2583.
- [8] J. Kluin, H. Talacua, A. I. P. M. Smits, M. Y. Emmert, M. C. P. Brugmans, E. S. Fioretta, P. E. Dijkman, S. H. M. Söntjens, R. Duijvelshoff, S. Dekker, M. W. J. T. Janssen-van den Broek, V. Lintas, A. Vink, S. P. Hoerstrup, H. M. Janssen, P. Y. W. Dankers, F. P. T. Baaijens, C. V. C. Bouten, *Biomaterials* **2017**, 125, 101.
- [9] D. E. Muylaert, J. O. Fledderus, C. V. Bouten, P. Y. Dankers, M. C. Verhaar, *Heart* **2014**, 100, 1825.
- [10] L. Hympanova, M. G. M. C. Mori da Cunha, R. Rynkevici, M. Zündel, M. R. Gallego, J. Vange, G. Callewaert, I. Urbankova, F. Van der Aa, E. Mazza, J. Deprest, *J. Mech. Behav. Biomed. Mater* **2017**, 74, 349.
- [11] S. Koudstaal, M. M. C. Bastings, D. A. M. Feyen, C. D. Waring, F. J. Van Slochteren, P. Y. W. Dankers, D. Torella, J. P. G. Sluijter, B. Nadal-Ginard, P. A. Doevendans, G. M. Ellison, S. A. J. Chamuleau, *J. Cardiovasc. Transl. Res.* **2014**, 7, 232.
- [12] M. H. Bakker, C. C. S. Tseng, H. M. Keizer, P. R. Seevinck, H. M. Janssen, F. J. Van Slochteren, S. A. J. Chamuleau, P. Y. W. Dankers, *Adv. Healthcare Mater.* **2018**, 7, 1.
- [13] P. Y. W. Dankers, M. J. A. van Luyn, A. Huizinga-van der Vlag, G. M. L. van Gemert, A. H. Petersen, E. W. Meijer, H. M. Janssen, A. W. Bosman, E. R. Popa, *Biomaterials* **2012**, 33, 5144.
- [14] M. C. P. P. Brugmans, S. H. M. Söntjens, M. A. J. J. Cox, A. Nandakumar, A. W. Bosman, T. Mes, H. M. Janssen, C. V. C. C. Bouten, F. P. T. T. Baaijens, A. Driessen-Mol, *Acta Biomater.* **2015**, 27, 21.
- [15] I. De Feijter, O. J. G. M. Goor, S. I. S. Hendrikse, M. Comellas-Aragonès, S. H. M. Söntjens, S. Zaccaria, P. P. K. H. Fransen, J. W. Peeters, L. G. Milroy, P. Y. W. Dankers, *Synlett* **2015**, 26, 2707.
- [16] R. E. Kieltyka, A. C. H. Pape, L. Albertazzi, Y. Nakano, M. M. C. Bastings, I. K. Voets, P. Y. W. Dankers, E. W. Meijer, *J. Am. Chem. Soc.* **2013**, 135, 11159.
- [17] M. T. Poldervaart, H. Gremmels, K. Van Deventer, J. O. Fledderus, F. C. Öner, M. C. Verhaar, W. J. A. Dhert, J. Alblas, *J. Controlled Release* **2014**, 184, 58.
- [18] Sui, H.; Kawakami, K.; Sakurai, N.; Hara, T.; Nohmi, T. **2009**, 31, 47.
- [19] S. L. Gooskens, T. D. Klasson, H. Gremmels, I. Logister, R. Pieters, E. J. Perlman, R. H. Giles, M. M. van den Heuvel-Eibrink, *Mol. Oncol.* **2017**, 12, 166.
- [20] H. Gremmels, O. G. De Jong, D. H. Hazenbrink, J. O. Fledderus, M. C. Verhaar, *Stem Cells Int.* **2017**, 2017, 1.
- [21] Carpentier, G. Angiogenesis Analyzer for ImageJ. <http://imagej.nih.gov/ij/macros/toolsets/Angiogenesis%20Analyzer.txt>.
- [22] W. Hirt, T. Nebe, C. Birr, *Wien Klin Wochenschr.* **1994**, 106, 250.
- [23] G. B. Wang, R. S. Labow, J. P. Santerre, *Macromolecules* **2000**, 33, 7321.
- [24] E. M. Christenson, J. M. Anderson, A. Hiltner, *J. Biomed. Mater. Res. - Part A* **2004**, 70, 245.
- [25] R. Matuo, F. G. Sousa, A. E. Escargueil, I. Grivicich, D. Garcia-Santos, J. A. B. Chies, J. Saffi, A. K. Larsen, J. A. Pêgas Henriquesa, *J. Appl. Toxicol.* **2009**, 29, 308.
- [26] P. Swann, T. Waters, D. Moulton, Y. Xu, Q. Zheng, M. Edwards, R. Mace, *Science (80-)* **1996**, 23, 1109.
- [27] P. Friedl, D. Gilmour, *Nat. Rev. Mol. Cell Biol.* **2009**, 10, 445.
- [28] M. G. Tonnesen, X. Feng, R. A. F. Clark, *J. Investig. Dermatol. Symp. Proc.* **2000**, 5, 40.
- [29] A. N. Clark, R. Youkey, X. Liu, L. Jia, R. Blatt, Y. J. Day, G. W. Sullivan, J. Linden, A. L. Tucker, *Circ. Res.* **2007**, 101, 1130.
- [30] S. Miura, K. Yamada, F. Kano, Y. Yoshimura, *Biol. Pharm. Bull.* **2004**, 27, 520.
- [31] L. Chung, D. R. Maestas, F. Housseau, J. H. Elisseeff, *Adv. Drug Delivery Rev.* **2017**, 114, 184.

SUPPORTING INFORMATION

Additional supporting information may be found online in the Supporting Information section at the end of this article.

How to cite this article: Besseling PJ, Mes T, Bosman AW, et al. The in-vitro biocompatibility of ureido-pyrimidinone compounds and polymer degradation products. *J Polym Sci.* 2021;59: 1267–1277. <https://doi.org/10.1002/pol.20210072>